frontiers | Frontiers in Chemistry

TYPE Original Research
PUBLISHED 27 September 2022
DOI 10.3389/fchem.2022.984069

OPEN ACCESS

EDITED BY
Frédéric Bihel Université de Strasbourg (CNRS), France

REVIEWED BY
Malliga Iyer,
National Institutes of Health (NIH), United States
David B. Finlay,
University of Otago, New Zealand

*CORRESPONDENCE
Francesca Gado,
francesca.gado@unimi.it
Clementina Manera,
clementina.manera@unipi.it
Grazia Chiellini,
grazia.chiellini@unipi.it

†PRESENT ADDRESS
Francesca Gado,
Department of Pharmaceutical Sciences, University of Milan, Milan, Italy

SPECIALTY SECTION
This article was submitted to Medicinal and Pharmaceutical Chemistry, a section of the journal Frontiers in Chemistry

RECEIVED 01 July 2022
ACCEPTED 05 September 2022
PUBLISHED 27 September 2022

CITATION
Ferrisi R, Gado F, Polini B, Ricardi C, Mohamed KA, Stevenson LA, Ortore G, Rapposelli S, Saccomanni G, Pertwee RG, Laprairie RB, Manera C and Chiellini G (2022), Design, synthesis and biological evaluation of novel orthosteric-allosteric ligands of the cannabinoid receptor type 2 (CB_2R). *Front. Chem.* 10:984069. doi: 10.3389/fchem.2022.984069

Design, synthesis and biological evaluation of novel orthosteric-allosteric ligands of the cannabinoid receptor type 2 (CB_2R)

Rebecca Ferrisi[1], Francesca Gado[1,2*†], Beatrice Polini[3], Caterina Ricardi[3], Kawthar A. Mohamed[4], Lesley A. Stevenson[5], Gabriella Ortore[1], Simona Rapposelli[1], Giuseppe Saccomanni[1], Roger G. Pertwee[5], Robert B. Laprairie[4,6], Clementina Manera[1,7*] and Grazia Chiellini[3,7*]

[1]Department of Pharmacy, University of Pisa, Pisa, Italy, [2]Department of Pharmaceutical Sciences, University of Milano Statale, Milan, Italy, [3]Department of Pathology, University of Pisa, Pisa, Italy, [4]College of Pharmacy and Nutrition, University of Saskatchewan, Saskatoon, SK, Canada, [5]School of Medicine, Medical Sciences and Nutrition, Institute of Medical Sciences, University of Aberdeen, Aberdeen, Scotland, United Kingdom, [6]Department of Pharmacology, College of Medicine, Dalhousie University, Halifax, NS, Canada, [7]CISUP, Centre for Instrumentation Sharing Pisa University, Pisa, Italy

It is well known that G protein–coupled receptors (GPCRs) assume multiple active states. Orthosteric ligands and/or allosteric modulators can preferentially stabilize specific conformations, giving rise to pathway-biased signaling. One of the most promising strategies to expand the repertoire of signaling-selective GPCR activators consists of dualsteric agents, which are hybrid compounds consisting of orthosteric and allosteric pharmacophoric units. This approach proved to be very promising showing several advantages over monovalent targeting strategies, including an increased affinity or selectivity, a bias in signaling pathway activation, reduced off-target activity and therapeutic resistance. Our study focused on the cannabinoid receptor type 2 (CB_2R), considered a clinically promising target for the control of brain damage in neurodegenerative disorders. Indeed, CB_2R was found highly expressed in microglial cells, astrocytes, and even in some neuron subpopulations. Here, we describe the design, synthesis, and biological evaluation of two new classes of potential dualsteric (bitopic) CB_2R ligands. The new compounds were obtained by connecting, through different linkers, the pharmacophoric portion of the CB_2R positive allosteric modulator (PAM), **EC21a**, with that of the CB_2R selective orthosteric agonist **LV62**, both developed in our laboratories. A preliminary screening enabled us to identify compound **JR64a** as the most promising of the series. Indeed, functional examination highlighted a signaling 'bias' in favor of G protein activation over βarrestin2 recruitment, combined with high affinity for CB_2R and the ability to efficiently prevent inflammation in human microglial cells (HMC3) exposed to LPS/TNFα stimulation, thus demonstrating great promise for the treatment of neurodegenerative diseases.

KEYWORDS

cannabinoid receptor type 2 (CB_2R), CB_2R allosteric modulators, dualsteric agents, antiinflammatory activity, human microglial cells

Introduction

Several neurodegenerative disorders display alterations in components of the endocannabinoid system (ECS), and a cannabinoid-based approach has proven efficacious in the reversal of certain neurodegenerative events in pre-clinical models of neuroinflammation, oxidative stress, and neuronal loss, among others (Basavarajappa et al., 2009; Di Marzo 2009; Aymerich et al., 2018; Mastinu et al., 2018). The ECS is a complex signaling system consisting of cannabinoid receptors, their endogenous ligands (known as "endocannabinoids"), and the enzymes responsible for endocannabinoid biosynthesis, cellular uptake and catabolism (Bisogno et al., 2005). The effects of endocannabinoids are primarily mediated by CB_1 and CB_2 cannabinoid receptors (CB_1Rs and CB_2Rs), which are G protein-coupled receptors (GPCRs), predominantly associated with $G\alpha_{i/o}$ proteins (Howlett et al., 2002). Their activation inhibits adenylyl cyclase and certain voltage dependent calcium channels, and regulates mitogen-activated protein kinase (MAPK) and phosphatidylinositol-3-kinase (PI3K) pathways (Howlett et al., 2002). CB_1Rs are highly expressed in the central nervous system (CNS) (Mackie 2005), where they play a well-established role in regulating neuronal excitability. In contrast, CB_2Rs have reduced expression in the brain compared to CB_1Rs. Indeed, the expression of CB_2R in the brain has been mainly identified at the level of microglia and vascular elements (Walter et al., 2003; Ramirez et al., 2012), and their modulation is not accompanied by psychotropic side effects associated with the activation of CB_1Rs.

Notably, activation of CB_2Rs results in inhibition of neuroinflammatory signaling pathways (Bie et al., 2018); therefore, this receptor type may be a clinically promising target for the control of brain damage in neurodegenerative disorders, including neuropathic pain, Alzheimer's disease, Parkinson's disease, Huntington's disease, and multiple sclerosis (Benito et al., 2003; Benito et al., 2005; Han et al., 2013; Chung et al., 2016; Xu et al., 2016; Ferrisi et al., 2021). However, to date only a few synthetic CB_2R agonists have reached an advanced stage of clinical trials (from ClinicalTrials.gov: GW842166X, S-777469, and JTE-907), probably because of the predominance of CB_2Rs on immune cells, whose activation might cause immunosuppression (Oláh et al., 2017).

Recent observations indicate that GPCRs are dynamic proteins able to assume multiple active states providing an interaction surface for intracellular adaptor proteins (e.g., heterotrimeric G proteins, G protein-coupled receptor kinases, and βarrestins) each of them responsible for different signaling pathway. Some ligands (orthosteric ligands or allosteric modulators) may stabilize a unique receptor conformation inducing a particular signaling pathway at the expense of others. This results in differential coupling to the signal transduction cascade and a biased response, a scenario which is also referred to as biased signaling or stimulus bias. Ligand bias should generate a biased response relatively independent of the cell system tested (Gurevich and Gurevich, 2019; Wootten et al., 2013; Smith et al., 2018). Biased GPCR ligands have been shown to display beneficial biological responses in preclinical and clinical studies, which explains the growing interests of medicinal chemists in biased signaling (Bock and Bermudez 2021). One of the most promising strategies to expand the repertoire of signaling-selective GPCR activators consists of dualsteric/bitopic agents, which are hybrid compounds composed of orthosteric and allosteric pharmacophoric units (Kamal and Jockers 2009; Lane et al., 2013). They bridge two topographically distinct ligand-binding domains, joining both orthosteric and allosteric properties within a single therapeutic agent. This strategy could offer access to GPCR modulators with a unique receptor subtype and signaling selectivity profile by virtue of targeting an allosteric site, as well as greater affinity due to the concomitant engagement with the orthosteric site. It is noteworthy that the special pharmacological profile of a bitopic ligand may be reflected in its unique binding kinetics. Theoretically, dualsteric ligands may have higher affinities than the respective partners. This may be derived from the ability of the two counterparts to bind into their corresponding binding pockets in an ideal manner without inducing an unfavorable conformational rearrangement of the receptor. In this view, upon binding, each pharmacophore has its own binding kinetics that can induce synergistic effects (i.e., allosteric cooperativity) on the overall kinetics of the bitopic ligand, greater than simply combining two individual components, as reported, for instance, for the M2 muscarinic receptor ligand, THR-160209 (Steinfeld et al., 2007). However, it may be expected that bitopic ligands do not always display an improved binding affinity; for example, a compromised binding affinity of the bitopic ligand can also occur when the individual pharmacophores have different preferences on receptor states (Antony et al., 2009). Bitopic/dualsteric ligands, may prove to be particularly useful in situations where endogenous agonist tone is progressively lost, such as in neurodegenerative disorders, thanks to the co-presence of the orthosteric and the allosteric modulator (Gentry et al., 2015). Finally, this innovative approach may also provide novel bias ligands because the

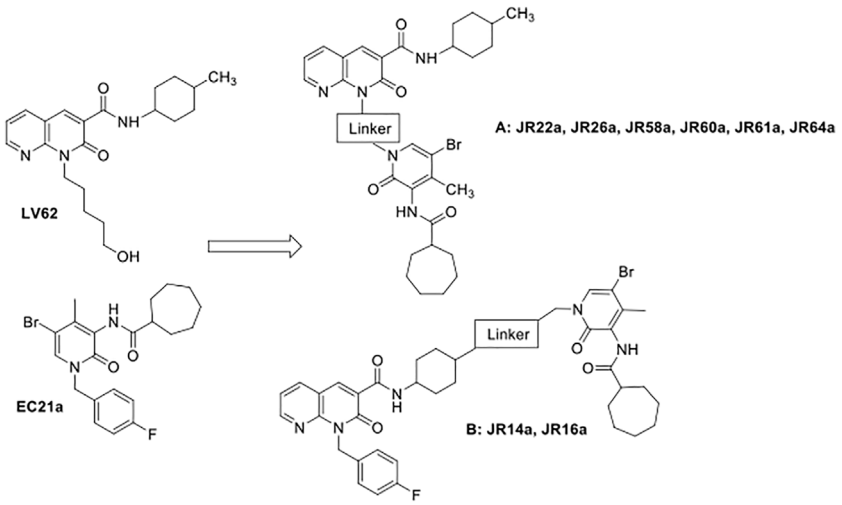

FIGURE 1
Design of potential CB_2R dualsteric ligands **(A)** and **(B)**.

incorporation of two pharmacophores in one ligand can severely impact receptor flexibility and thus signaling output (Lane et al., 2013; Schrage and Kostenis 2017; Reinecke et al., 2019).

Here, we describe the design, synthesis, and biological evaluation of potential CB_2R dualsteric ligands, characterized by general structures **A** and **B** (Figure 1). The two classes of compounds were obtained by connecting, through different linkers, the pharmacophoric portion of a previously identified CB_2R positive allosteric modulator (PAM), namely **EC21a** (Gado et al., 2019; Shapiro et al., 2021), with that of the CB_2R selective orthosteric agonist **LV62**, which belongs to the class of 1,8-naphthyridin-2(1*H*)-one-3-carboxamide derivatives, previously identified by us as potent CB_2R orthosteric agonists (Lucchesi et al., 2014). The nitrogen atom in position 1 and the 4-methyl cyclohexyl group in position 3 of **LV62** moiety were selected to connect in position N (1) of the central core of **EC21a**, obtaining respectively the **A** (**JR22a, JR26a, JR58a, JR60a, JR61a, JR64a** compounds) and **B** (**JR14a, JR16a** compounds) series. Previous structural activity relation (SAR) studies on 1,8-naphthyridin-2(1*H*)-one-3-carboxamide derivatives (Lucchesi et al., 2014; Cooper et al., 2018) and on **EC21a** analogues (Gado et al., 2019; Gado et al., 2021) indicated these positions as the most suitable to chemical modifications without significantly compromising activity. The choice of the correct linker plays a crucial role in allowing the two pharmacophores to interact correctly with the respective binding site. Obviously, a deep knowledge of the orthosteric and allosteric binding sites will make easier the choice (Newman et al., 2020). The orthosteric CB_2R binding site is well known now (Li et al., 2019), on the contrary there are no reliable structural data about the allosteric binding site of the CB_2R. For this reason, the linkers used to obtain our ligands have been chosen on the basis of what previously reported for the bivalent/bitopic ligand (Kamal and Jockers. 2009; Newman et al., 2020; Meijer et al., 2021; Obeng et al., 2021; Gado et al., 2022).

A preliminary screening of the newly designed dualsteric CB_2R ligands, led to the identification of compound **JR64a** as the most promising bitopic/dualsteric CB_2R ligand of the series. Indeed, a signaling 'bias' in favor of G protein activation over βarrestin2 recruitment was observed, combined with high binding affinity for CB_2R. Functional examination highlighted the ability of this compound to efficiently prevent inflammation in human microglial cells (HMC3) exposed to LPS/TNFα stimulation, as demonstrated by the reduced secretion of pro-inflammatory IL-6 and increased secretion of anti-inflammatory IL-10.

Materials and methods

Chemistry

Commercially available reagents were purchased from Sigma Aldrich, Tokyo Chemical Industry or Fluorochem and used without purification. ^{1}H NMR and ^{13}C NMR were recorded at 400 and 100 MHz respectively, on a Bruker AVANCE IIITM 400 spectrometer. Chemical shift (δ) is reported in parts per million related to the residual solvent signal, while coupling constants (J) are expressed in Hertz (Hz). All compounds are >95% pure by HPLC analysis. The analytical HPLC system consisted of a Varian 9,012 Solvent Delivery System,

coupled to a Varian ProStar 330 DAD detector with operating wavelengths in the range between 200 and 400 nm, and the Star LC Workstation version 6.41 software was used for instrument control, data acquisition, and data processing. Analyses were performed on a reverse phase C18 column (Luna C18 (2) 150 mm × 4.6 mm, 5 µm particle size, Phenomenex®). The mobile phase was constituted by H_2O (eluent A) and ACN (eluent B) at a flow rate of 600 µL/min. A linear gradient starting from 40% of A, changing to 80% of A over 30 min, and returning to the initial conditions over 20 min was used. The target compounds are ≥97% pure by HPLC analysis (Supporting Information). High resolution mass spectra (HRMS) were recorded on a Q Exactive™ Plus Hybrid Quadrupole-Orbitrap™ Mass Spectrometer (Thermo Fisher Scientific), equipped with HESI source. The ESI-MS spectrum was recorded by direct injection at 5 µml min- 1 flow rate. Working conditions: positive polarity, spray voltage 3.5 kV, capillary temperature 300°C, S-lens RF level 55, sheath gas 20, auxiliary gas 3 (arbitrary units); negative polarity, spray voltage 3.4 kV, capillary temperature 270°C, S-lens RF level 55, sheath gas 35, auxiliary gas 8 (arbitrary units). Acquisition and analysis: Xcalibur 4.2 software (Thermo). For spectra acquisition a nominal resolution (at m/z 200) of 140,000 was used. Organic solutions were dried over anhydrous Na_2SO_4. Evaporation was carried out in vacuo using a rotating evaporator. Silica gel flash chromatography was performed using silica gel 60 Å (0.040–0.063 mm; Merck Life Science S. r.l.). Reactions were monitored by TLC on Merck aluminium silica gel (60 F254) plates that were visualized under a UV lamp (λ = 254 nm). Melting points were determined on a Kofler hot-stage apparatus and are uncorrected.

The synthesis of the precursors of JR compounds is reported in Supporting Information.

N-(4-(5-(4-(3-(5-bromo-3-(cycloheptanecarboxamido)-4-methyl -2-oxopyridin-1(2*H*)-yl)propyl)-1*H*-1,2,3-triazol-1-yl) pentanamido)cyclohexyl)-1-(4-fluorobenzyl)-2-oxo-1,2-dihydro-1,8-naphthyridine-3-carboxamide (JR14a). To a solution of compounds **5** (40.0 mg, 0.08 mmol) and **15** (31.5 mg, 0.08 mmol) in DMF (1.71 ml) and water (0.85 ml), $CuSO_4.5H_2O$ (20.0 mg, 0.08 mmol) and sodium ascorbate (47.6 mg, 0.24 mmol) were added. The reaction mixture was stirred at 80°C for 2 h. Subsequently, the solvent was removed under reduced pressure to give a residue which was dissolved in ethyl acetate and washed with saturated solution of $NaHCO_3$. The organic phase was dried over Na_2SO_4, filtered, and evaporated under reduced pressure. The crude product obtained was purified by flash chromatography on silica gel using, firstly, ethyl acetate and 5% of methanol, and then ethyl acetate and 10% of methanol as eluent to afford compound **JR14a** (36.5 mg, 0.04 mmol) as a brownish solid. Yield: 50%. Mp: 108°C (dec.). ^{1}H-NMR ($CDCl_3$) δ (ppm) 9.90 (bd, 1H, *J* = 7.2 Hz, NH), 8.90 (s, 1H, H_4), 8.72 (dd, 1H, *J* = 4.6 Hz; 1.8 Hz, H_7), 8.10 (dd, 1H, *J* = 7.8 Hz; 1.8 Hz, H_5), 7.55 (bs, 1H, NH), 7.43 (m, 3H, Ar-H + H_6-Py), 7.37 (s, 1H, NCHC), 7.30 (dd, 1H, *J* = 7.8 Hz; 4.6 Hz, H_6), 6.96 (AA'XX' system, 2H, Ar-H), 5.78 (s, 2H, CH_2), 5.63 (bd, 1H, *J* = 7.6 Hz, NH), 4.35 (t, 2H, *J* = 7.0 Hz, CH_2-triazole), 4.20 (m, 1H, CHN), 3.99 (t, 2H, *J* = 7.0 Hz, CH_2NCO), 3.93 (m, 1H, CH), 2.75 (t, 2H, *J* = 7.2 Hz, CH_2-triazole), 2.51 (m, 1H, CHCO), 2.20 (t, 2H, *J* = 7.2 Hz, CH_2CONH), 2.14 (s, 3H, CH_3), 1.84 (m, 26H, cyclohexyl + cycloheptyl + 3xCH_2). ^{13}C-NMR ($CDCl_3$) δ (ppm) 176.11, 171.45, 162.87, 161.97, 162.22 (d, *J* = 245 Hz), 158.43, 152.30, 149.80, 146.50, 142.47, 142.23, 138.70, 133.10, 132.81 (d, *J* = 3 Hz), 130.29 (d, *J* = 8 Hz), 126.38, 123.31, 121.21, 119.56, 115.35 (d, *J* = 21 Hz), 115.10, 103.46, 49.92, 49.34, 47.85, 46.38, 45.54, 44.16, 35.78, 31.81, 29.72, 28.63, 28.55, 28.48, 28.24, 26.69, 22.56, 22.50, 20.43. HRMS-ESI: m/z calcd for $C_{46}H_{55}BrFN_9O_5$ $[M-H]^-$, 910.34208; found 910.34450.

N-(4-(5-(4-((5-bromo-3-(cycloheptanecarboxamido)-4-methyl-2-oxopyridin-1(2*H*)-yl)methyl)-1*H*-1,2,3-triazol-1-yl)pentanamido)cyclohexyl)-1-(4-fluorobenzyl)-2-oxo-1,2-dihydro-1,8-naphthyridine-3-carboxamide (JR16a). Compound **JR16a** was prepared from compounds **5** and **16** as described for compound **JR14a** and purified by flash column chromatography on a silica gel using ethyl acetate and 10% of methanol. Yield: 55%. Mp: 113 °C (dec.). ^{1}H-NMR ($CDCl_3$) δ (ppm) 9.90 (bd, 1H, *J* = 7.6 Hz, NH), 8.91 (s, 1H, H_4), 8.72 (dd, 1H, *J* = 4.8 Hz; 2.0 Hz, H_7), 8.10 (dd, 1H, *J* = 7.8 Hz; 2.0 Hz, H_5), 7.67 (s, 1H, NCHC), 7.64 (bs, 1H, NH), 7.46 (m, 3H, Ar-H + H_6-Py), 7.31 (dd, 1H, *J* = 7.8 Hz; 4.8 Hz, H_6), 6.97 (AA'XX' system, 2H, Ar-H), 5.79 (s, 2H, CH_2), 5.56 (bd, 1H, *J* = 7.6 Hz, NH), 5.15 (s, 2H, CCH_2N), 4.35 (t, 2H, *J* = 7.4 Hz, CH_2-triazole), 4.21 (m, 1H, CHN), 3.95 (m, 1H, CH), 2.50 (m, 1H, CHCO), 2.19 (t, 2H, *J* = 7.6 Hz, CH_2CONH), 2.13 (s, 3H, CH_3), 1.84 (m, 24H, cyclohexyl + cycloheptyl + 2xCH_2). ^{13}C-NMR ($CDCl_3$) δ (ppm) 176.14, 171.45, 162.85, 162.17 (d, *J* = 245 Hz), 161.96, 158.25, 152.32, 149.75, 143.33, 142.53, 142.03, 138.72, 133.06, 132.75 (d, *J* = 3 Hz), 130.19 (d, *J* = 9 Hz), 126.17, 123.90, 123.23, 119.58, 115.32 (d, *J* = 22 Hz), 115.08, 103.91, 50.15, 47.73, 46.28, 45.54, 44.52, 44.14, 35.67, 31.77, 29.55, 28.58, 28.52, 28.19, 26.66, 22.54, 20.37. HRMS-ESI: m/z calcd for $C_{44}H_{51}BrFN_9O_5$ $[M-H]^-$, 882.31075; found 882,31,397.

1-(5-(4-(3-(5-bromo-3-(cycloheptanecarboxamido)-4-methyl-2-oxopyridin-1(2*H*)-yl)propyl)-1*H*-1,2,3-triazol-1-yl)pentyl)-*N*-(4-methylcyclohexyl)-2-oxo-1,2-dihydro-1,8-naphthyridine-3-carboxamide (JR22a). Compound **JR22a** was prepared from compounds **7** and **15** as described for compound **JR14a** and purified by flash column chromatography on a silica gel using ethyl acetate and 10% of methanol. Yield: 58%. Mp: 114 °C (dec.). ^{1}H-NMR ($CDCl_3$) δ (ppm) 9.96 and 9.60 (2d, 1H, *J* = 7.2 Hz, NH), 8.87 (s, 1H, H_4), 8.70 (dd, 1H, *J* = 4.8 Hz; 2.0 Hz, H_7), 8.08 (dd, 1H, *J* = 7.8 Hz; 2.0 Hz, H_5), 7.47 (bs, 1H, NH), 7.44 (s, 1H, NCHC), 7.41 (s, 1H, H_6-Py), 7.28 (dd, 1H, *J* = 7.8 Hz; 4.8 Hz, H_6), 4.57 (2t, 2H, *J* = 7.6 Hz, CH_2NCO), 4.38 (t, 2H, *J* = 7.2 Hz, CH_2-triazole), 4.25 and 3.92 (2m, 1H, CH), 4.02 (t, 2H, *J* = 7.2 Hz, CH_2NCO), 2.78 (t, 2H, *J* = 7.2 Hz, CH_2-triazole), 2.50 (m, 1H, CHCO), 2.15 (s, 3H, CH_3), 1.59 (m, 29H, cyclohexyl + cycloheptyl + 4xCH_2), 0.97 and 0.92 (2d,

3H, *J* = 6.4 Hz, CH_3). ^{13}C-NMR ($CDCl_3$) δ (ppm) 176.10, 162.56, 161.96, 158.37, 152.12, 149.65, 146.46, 142.23, 142.00, 138.55, 133.09, 126.32, 123.14, 120.98, 119.15, 114.99, 103.44, 50.12, 49.36, 48.87, 47.77, 41.51, 33.94, 33.02, 32.04, 31.75, 29.96, 28.48, 28.18, 27.18, 26.64, 24.04, 22.46, 22.28, 20.42. HRMS-ESI: m/z calcd for $C_{40}H_{53}BrN_8O_4$ M-H]$^-$, 787.33003; found 787.33307.

1-(5-(4-((5-bromo-3- (cycloheptanecarboxamido)-4-methyl-2-oxopyridin-1(2*H*)-yl)methyl)-1*H*-1,2,3-triazol-1-yl)pentyl)-*N*-(4-methylcyclohexyl) -2-oxo-1,2-dihydro-1,8-naphthyridine-3-carboxamide (JR26a). Compound **JR26a** was prepared from compounds **7** and **16** as described for compound **JR14a** and purified by flash column chromatography on a silica gel using ethyl acetate and 10% of methanol. Yield: 59%. Mp: 116 °C (dec.). ^{1}H-NMR ($CDCl_3$) δ (ppm) 9.98 and 9.59 (2d, 1H, *J* = 7.2 Hz, NH), 8.86 (s, 1H, H_4), 8.69 (dd, 1H, *J* = 4.8 Hz; 2.0 Hz, H_7), 8.07 (dd, 1H, *J* = 7.8 Hz; 2.0 Hz, H_5), 7.66 (s, 1H, NCHC), 7.64 (bs, 1H, NH), 7.39 (s, 1H, H_6-Py), 7.27 (dd, 1H, *J* = 7.8 Hz; 4.8 Hz, H_6), 5.17 (s, 2H, CCH_2N), 4.57 (2t, 2H, *J* = 7.6 Hz, CH_2NCO), 4.35 (t, 2H, *J* = 7.4 Hz, CH_2-triazole), 4.25 and 3.90 (2m, 1H, CH), 2.49 (m, 1H, CHCO), 2.14 (s, 3H, CH_3), 1.56 (m, 27H, cyclohexyl + cycloheptyl + 3xCH_2), 0.97 and 0.90 (2d, 3H, *J* = 6.6 Hz, CH_3). ^{13}C-NMR ($CDCl_3$) δ (ppm) 176.00, 162.62, 161.95, 158.16, 152.11, 149.73, 142.84, 142.00, 141.83, 138.51, 132.86, 126.13, 123.64, 123.28, 119.12, 114.99, 103.88, 50.41, 47.84, 45.74, 44.44, 41.42, 31.78, 31.09, 30.27, 29.87, 29.65, 28.17, 27.14, 26.66, 24.03, 21.58, 20.48. HRMS-ESI: m/z calcd for $C_{38}H_{49}BrN_8O_4$ M-H]-, 759.29873; found 759.29901.

1-(5-(5-bromo-3-(cycloheptanecarboxamido)-4- methyl-2-oxopyridin-1(2H)-yl)pentyl)-N- (4-methylcyclohexyl)-2-oxo-1,2-dihydro-1,8-naphthyridine-3-carboxamide (JR61a). NaH (60% dispersion in mineral oil) (8.4 mg, 0.21 mmol) was added portion wise at 0°C to a solution of compound **14** (70 mg, 0.21 mmol) in DME (0.4 ml) and anhydrous DMF (0.1 ml). LiBr (36.5 mg, 0.42 mmol) was added 15 min later. The mixture was stirred for 20 min at room temperature. Compound **6** (182 mg, 0.42 mmol), as a mixture of 1:1 *trans* and *cis* isomers, was added dropwise, and the reaction was stirred at 65°C overnight. Solvents were removed under reduced pressure. The mixture obtained was dissolved in $CHCl_3$ and washed three times with water. The organic phase was dried over Na_2SO_4, filtered, and evaporated under reduced pressure. The crude product obtained was purified by flash chromatography on silica gel using hexane/AcOEt 5:5 as eluent to afford compound **JR61a** (33.0 mg, 0.05 mmol) as a yellowish solid. Yield: 24%. Mp: 118 °C (dec.). ^{1}H-NMR ($CDCl_3$) δ (ppm) 9.98 and 9.62 (2d, 1H, *J* = 7.8 Hz, NH), 8.85 (s, 1H, H_4), 8.69 (dd, 1H, *J* = 4.4 Hz; 1.6 Hz, H_7), 8.06 (dd, 1H, *J* = 7.8 Hz; 1.6 Hz, H_5), 7.56 (bs, 1H, NH), 7.34 (s, 1H, H_6-Py), 7.26 (dd, 1H, *J* = 7.8 Hz; 4.4 Hz, H_6), 4.57 (2t, 2H, *J* = 7.6 Hz, CH_2NCO), 4.24 and 3.89 (2m, 1H, CH), 3.91 (t, 2H, *J* = 7.4 Hz, CH_2NCO), 2.50 (m, 1H, CHCO), 2.15 (s, 3H, CH_3), 1.58 (m, 27H, cyclohexyl + cycloheptyl + 3xCH_2), 0.96 and 0.90 (2d, 3H, *J* = 6.4 Hz, CH_3). ^{13}C-NMR ($CDCl_3$) δ (ppm) 175.95, 162.44, 161.82, 158.08, 151.95, 149.58, 141.80, 141.63, 138.38, 132.54, 126.27, 123.09, 118.96, 114.83, 103.35, 49.97, 48.69, 47.63, 45.56, 41.36, 33.80, 32.87, 31.88, 31.59, 30.94, 30.10, 29.49, 28.68, 28.03, 27.14, 26.49, 23.90, 22.14, 21.41, 20.32. HRMS-ESI: m/z calcd for $C_{35}H_{46}BrN_5O_4$ M-H]$^-$, 678.26604; found 678.26887.

1-(7-(5-bromo-3-(cycloheptanecarboxamido)-4-methyl-2-oxopyridin-1(2H)-yl)heptyl)-N-(4-methylcyclohexyl)-2-oxo-1,2-dihydro-1,8-naphthyridine-3-carboxamide (JR64a). Compound **JR64a** was prepared from compounds **14** and **8** as described for compound **JR61a** and purified by flash column chromatography on a silica gel using hexane/AcOEt 5:5. Yield: 18%. Mp: 121 °C (dec.). ^{1}H-NMR ($CDCl_3$) δ (ppm) 10.01 and 9.65 (2d, 1H, *J* = 7.6 Hz, NH), 8.85 (s, 1H, H_4), 8.69 (dd, 1H, *J* = 4.6 Hz; 1.8 Hz, H_7), 8.06 (dd, 1H, *J* = 7.8 Hz; 1.8 Hz, H_5), 7.49 (bs, 1H, NH), 7.31 (s, 1H, H_6-Py), 7.26 (dd, 1H, *J* = 7.8 Hz; 4.6 Hz, H_6), 4.54 (2t, 2H, *J* = 7.8 Hz, CH_2NCO), 4.24 and 3.92 (2m, 1H, CH), 3.88 (t, 2H, *J* = 7.4 Hz, CH_2NCO), 2.50 (m, 1H, CHCO), 2.15 (s, 3H, CH_3), 1.60 (m, 31H, cyclohexyl + cycloheptyl + 5xCH_2), 0.97 and 0.91 (2d, 3H, *J* = 6.4 Hz, CH_3). ^{13}C-NMR ($CDCl_3$) δ (ppm) 176.13, 162.68, 162.12, 158.25, 152.12, 149.84, 141.93, 141.75, 138.56, 132.65, 126.45, 123.33, 119.08, 115.05, 103.63, 50.29, 48.92, 47.93, 45.83, 42.03, 41.93, 34.03, 33.09, 32.12, 31.82, 30.32, 29.67, 29.30, 29.00, 28.25, 27.88, 26.99, 26.94, 26.71, 26.62, 22.36, 20.56. HRMS-ESI: m/z calcd for $C_{37}H_{50}BrN_5O_4$ M-H]$^-$, 706.29734; found 706.29881.

1-(2-(2-(5-bromo-3-(cycloheptanecarboxamido)-4-methyl-2-oxopyridin-1(2H)-yl)ethoxy)ethyl)-N-(4-methylcyclohexyl)-2-oxo-1,2-dihydro-1,8-naphthyridine-3-carboxamide (JR58a). Compound **JR58a** was prepared from compounds **14** and **9** as described for compound **JR61a** and purified by flash column chromatography on a silica gel using hexane/AcOEt 3:7. Yield: 59%. Mp: 110 °C (dec.). ^{1}H-NMR ($CDCl_3$) δ (ppm) 9.95 and 9.60 (2d, 1H, *J* = 7.6 Hz, NH), 8.84 (s, 1H, H_4), 8.60 (dd, 1H, *J* = 4.6 Hz; 2.0 Hz, H_7), 8.02 (dd, 1H, *J* = 7.6 Hz; 2.0 Hz, H_5), 7.66 (bs, 1H, NH), 7.31 (s, 1H, H_6-Py), 7.25 (dd, 1H, *J* = 7.6 Hz; 4.6 Hz, H_6), 4.80 (m, 2H, CH_2NCO), 4.20 and 3.85 (2m, 1H, CH), 4.00 (m, 2H, CH_2NCO), 3.80 (m, 2H, OCH_2), 3.73 (m, 2H, OCH_2), 2.48 (m, 1H, CHCO), 2.14 (s, 3H, CH_3), 1.56 (m, 21H, cyclohexyl + cycloheptyl), 0.92 and 0.87 (2d, 3H, *J* = 6.4 Hz, CH_3). ^{13}C-NMR ($CDCl_3$) δ (ppm) 175.99, 162.68, 161.75, 158.15, 151.80, 149.75, 142.11, 141.98, 138.36, 133.99, 125.84, 123.33, 119.16, 114.74, 102.73, 68.43, 67.99, 49.35, 48.74, 47.60, 45.83, 40.48, 40.42, 33.79, 32.88, 31.88, 31.61, 30.10, 29.52, 28.03, 26.49, 22.10, 21.41, 20.24. HRMS-ESI: m/z calcd for $C_{34}H_{44}BrN_5O_5$ M-H]$^-$, 680,24,530; found 680.24717.

1-(4-(4-(5-bromo-3-(cycloheptanecarboxamido)-4-methyl-2-oxopyridin-1(2H)-yl)butoxy) butyl)-N-(4-methylcyclohexyl)-2-oxo-1,2-dihydro-1,8-naphthyridine-3-carboxamide (JR60a). Compound **JR60a** was prepared from compounds **14** and **10** as described for compound **JR61a** and purified by flash column

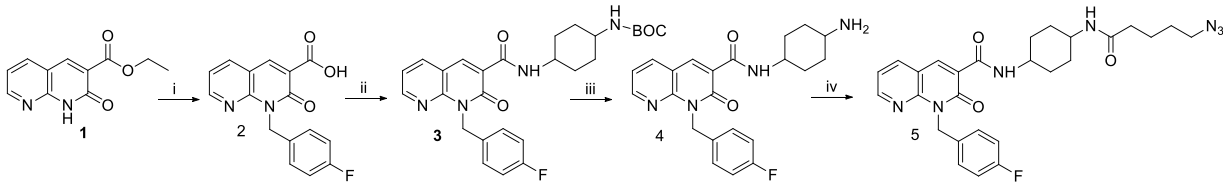

SCHEME 1
Synthetic pathway for the synthesis of the intermediate **5.** Reagents and conditions: i) a) DMF, Cs_2CO_3, 1h, rt; b) *p*-fluorobenzyl bromide, 50°C, 12h; c) NaOH 10%, 100°C, 24 h; ii) a) DMF, NEt_3, TBTU, 0°C, 30 min.; b) *cis*-4-(Boc-amino) cyclohexylamine, 0°C, 30 min.; c) rt, 12 h; iii) CH_2Cl_2, CF_3COOH, −20°C, 3h; iv) a) 5-azidopentanoic acid, DMF, NEt_3, TBTU, 0°C, 30 min.; b) compound **4**, 0°C, 30 min.; c) rt, 12h.

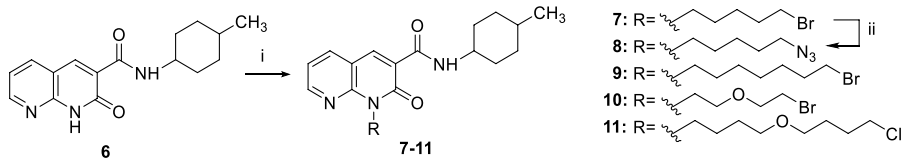

SCHEME 2
Synthetic pathway for the synthesis of the intermediates **7-11.** Reagents and conditions: *i*) a) CsF, DMF, rt, 1h; b) suitable R-Br or R-Cl, 30 °C, 24 h; *ii*) NaN_3, DMF, 60 °C, 12 h.

chromatography on a silica gel using hexane/AcOEt 3:7. Yield: 12%. Mp: 118 °C (dec.). ^{1}H-NMR ($CDCl_3$) δ (ppm) 10.01 and 9.65 (2d, 1H, *J* = 7.2 Hz, NH), 8.85 (s, 1H, H_4), 8.66 (dd, 1H, *J* = 4.6 Hz; 1.4 Hz, H_7), 8.05 (dd, 1H, *J* = 7.6 Hz; 1.4 Hz, H_5), 7.51 (bs, 1H, NH), 7.34 (s, 1H, H_6-Py), 7.24 (dd, 1H, *J* = 7.6 Hz; 4.6 Hz, H_6), 4.61 (2t, 2H, *J* = 7.6 Hz, CH_2NCO), 4.25 and 3.88 (2m, 1H, CH), 3.93 (t, 2H, *J* = 6.8 Hz, CH_2NCO), 3.46 (m, 4H, 2xOCH_2), 2.50 (m, 1H, CHCO), 2.14 (s, 3H, CH_3), 1.58 (m, 29H, cyclohexyl + cycloheptyl, 4xCH_2), 0.97 and 0.91 (2d, 3H, *J* = 6.4 Hz, CH_3). ^{13}C-NMR ($CDCl_3$) δ (ppm) 175.98, 162.50, 161.92, 158.15, 151.95, 149.67, 141.80, 141.62, 138.34, 132.70, 126.17, 123.07, 118.93, 114.84, 103.28, 70.42, 70.25, 49.83, 48.72, 47.66, 45.58, 44.91, 41.65, 33.81, 32.87, 31.90, 31.60, 30.09, 29.60, 28.03, 27.16, 27.12, 26.52, 26.49, 24.73, 22.60, 21.41, 20.24. HRMS-ESI: m/z calcd for $C_{38}H_{52}BrN_5O_5$ M-H]$^-$, 736,30,788; found 736.30861.

Cell cultures and reagents

CP55,940 was purchased from Cayman Chemicals (Ann Arbor, MI) [^{3}H]CP55,940 at a concentration of 174.6 Ci/mmol was purchased from PerkinElmer (Guelph, ON). LPS (*Escherichia coli* 0111:B4) and TNFα were purchased from Sigma-Aldrich (Milan, Italy), whereas SR144528 was from Tocris (Bristol, United Kingdom). Chinese hamster ovary (CHO)-K1 cells originally obtained from ATCC (Catalog No. CCL-61, Manassas, VA) stably expressing human cannabinoid CB_1R (*h*CB_1R) or CB_2R (*h*CB_2R) described previously were maintained at 37°C, 5% CO_2 in F-12 DMEM containing 1 mM l-glutamine, 10% FBS, and 1% Pen/Strep as well as hygromycin B (300 μg/ml) and G418 (600 μg/ml) for CHO-K1 *h*CB_1R cells or G418 (400 μg/ml) for CHO-K1 *h*CB_2R cells (Garai et al., 2020; Zagzoog et al., 2020). In the case of membrane collection for radioligand binding, cells were removed from flasks by scraping, centrifuged, and then frozen as a pellet at -80°C until required. Before use in a radioligand binding assay, cells were defrosted, diluted in Tris buffer (50 mM Tris [pH 7.4]) and homogenized with a 1 ml hand-held homogenizer. HitHunter® (cAMP) and PathHunter® (βarrestin2) CHO-K1 cells stably-expressing *h*CB_2R from DiscoveRx (Eurofins, Fremont, CA) were maintained at 37 °C, 5% CO_2 in F-12 DMEM containing 10% FBS and 1% Pen/Strep with 800 μg/ml geneticin (HitHunter®) or 800 μg/ml G418 and 300 μg/ml hygromycin B (PathHunter®), as previously reported (Garai et al., 2020; Zagzoog et al., 2020). The human microglial clone 3 cell line (HMC3) (ATCC® CRL-3304™) was cultured in high glucose DMEM supplemented with 10% FBS, streptomycin (100 g/ml) and penicillin (100 U/mL) (Sigma-Aldrich, Milan, Italy).

HitHunter® cAMP assay

Inhibition of FSK-stimulated cAMP accumulation was measured using the DiscoveRx HitHunter assay. Twenty thousand cells/well were plated in low-volume 96-well plates and incubated overnight in Opti-MEM containing 1% FBS at 37°C and 5% CO_2. Opti-MEM media was then removed and replaced with cell

10.3389/fchem.2022.984069

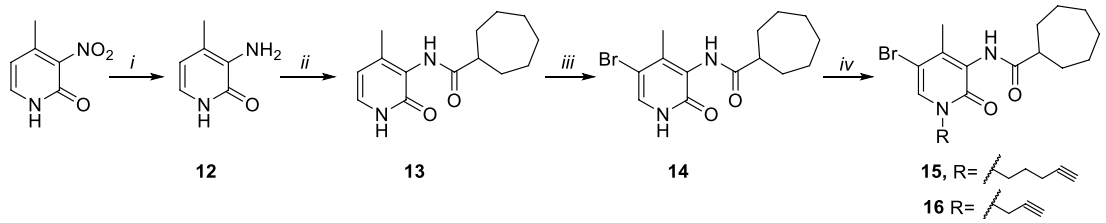

SCHEME 3
Synthetic pathway for the synthesis of the alkyne derivatives **15** and **16.** Reagents and conditions: i) Fe, NH_4Cl, H_2O/EtOH 1:2, 80 °C, 3 h. ii) a) cycloheptanecarboxylic acid, $C_2O_2Cl_2$, DMF, rt, 0.5 h b) NEt_3, DCM, DMF, rt, 24 h. iii) Br_2, $CHCl_3$, rt, 12 h. iv) a) CsF, DMF, rt, 1 h b) R-bromide, 30°C, 12h.

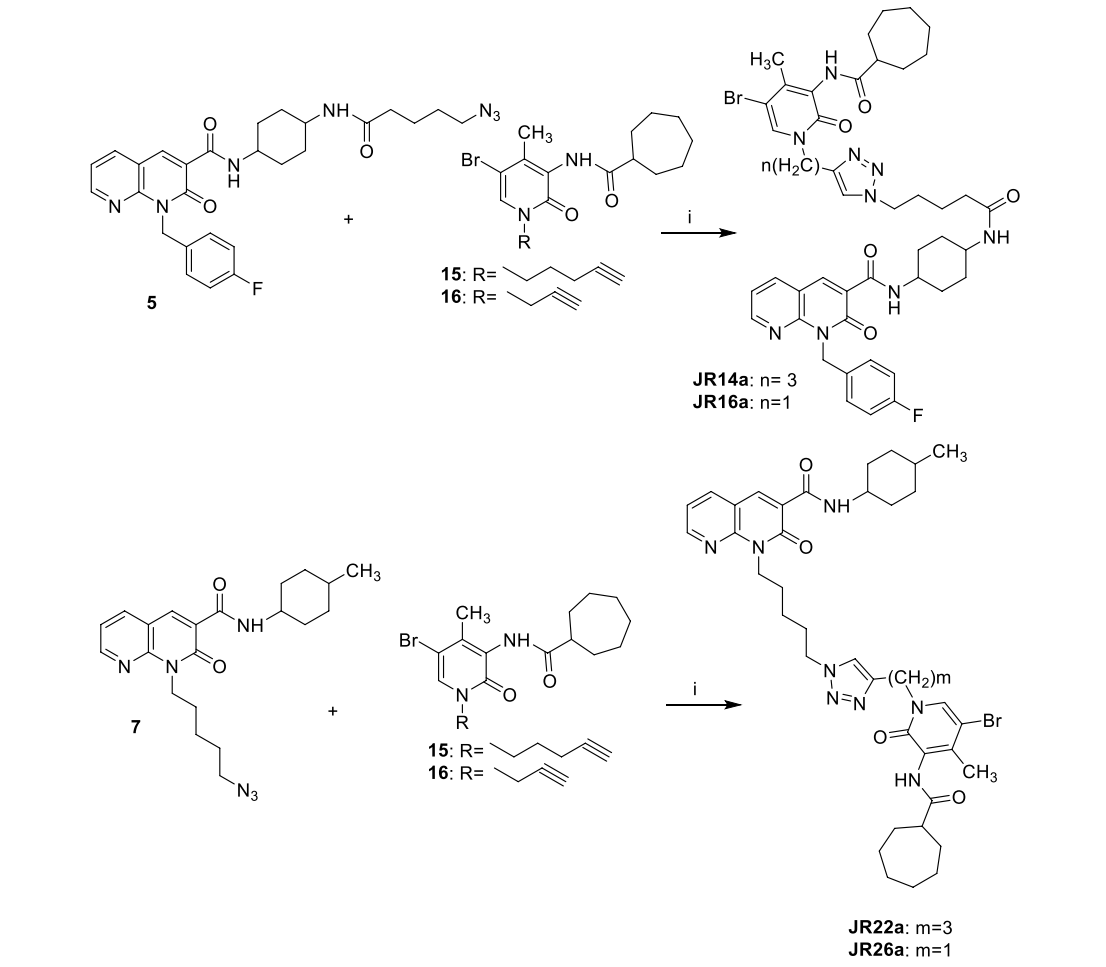

SCHEME 4
Synthetic pathway for the synthesis of compounds **JR14a, JR16a** and **JR22a**, **JR26a** Reagents and conditions: *i)* $CuSO_4{\cdot}5H_2O$, sodium ascorbate, DMF/H_2O 4:1, 80°C, 2 h.

assay buffer (DiscoveRx) and cells were co-treated at 37°C with 10 μM FSK and ligands for 90 min cAMP antibody solution and cAMP working detection solutions were added to cells (DiscoveRx), and cells were incubated for 60 min at room temperature. cAMP solution A (DiscoveRx) was added, and cells were incubated for an additional 180 min at room temperature before chemiluminescence was measured on a Cytation5 plate reader (top read, gain 200, integration time 10,000 ms).

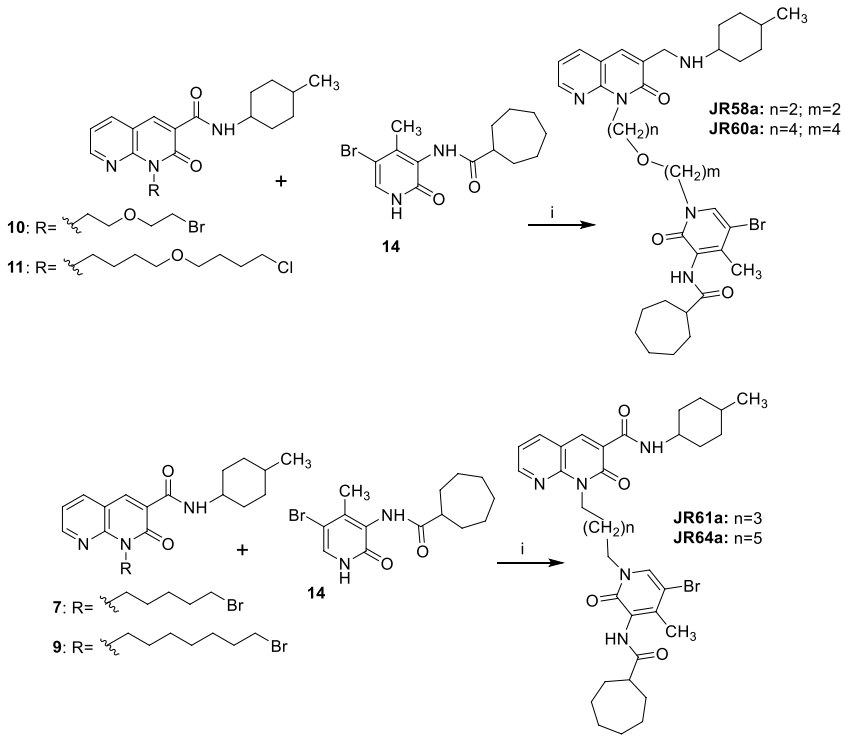

SCHEME 5
Synthetic pathway for the synthesis of compounds **JR58a**, **JR60a**, **JR61a** and **JR64a**. Reagents and conditions: *i)* a) NaH, DME, DMF, 0°C, 30 min; b) LiBr r.t. 20 min; suitable c) 65 °C, 12 h.

PathHunter® βarrestin2 assay

βarrestin2 recruitment was quantified using the DiscoveRx PathHunter® assay. Cells (20,000 cells/well in low-volume 96-well plates) were incubated overnight in Opti-MEM containing 1% FBS at 37 °C and 5% CO_2. Cells were treated with ligands for 90 min at 37 °C. Detection solution was added to cells (DiscoveRx), and cells were incubated for 60 min at room temperature. Chemiluminescence was measured on a Cytation5 plate reader (top read, gain 200, integration time 10,000 ms).

Radioligand displacement assay

CHO-K1 cells were thawed, diluted in Tris buffer (50 mM Tris [pH 7.4]) and homogenized in a 1 ml hand-held homogenizer. *h*CB_1R and *h*CB_2R CHO-K1 cell membranes were collected by cavitation in a pressure cell, and sedimented by ultracentrifugation. Pellets were resuspended in TME buffer (50 mM Tris, 5 mM $MgCl_2$, 1 mM EDTA [pH 7.4]), and protein concentration was measured via the Bradford method according to the manufacturer's directions (Bio-Rad Laboratories, Mississauga, ON). Competition binding experiments were conducted with 1 nM [^{3}H]CP55,940 and Tris binding buffer (50 mM Tris, 0.1% BSA [pH 7.4], 2 ml). Radioligand binding began with the addition of CHO-K1 cell membranes (25 µg protein per sample). Assays were performed for 120 min at 37°C and stopped by the addition of ice-cold Tris binding buffer (pH 7.4), followed by vacuum filtration using a 24-well sampling manifold (Brandel Cell Harvester; Brandel Inc., Gaithersburg, MD, United States). Brandel GF/B filter paper was soaked with wash buffer at 4 °C for at least 24 h. Each filter paper was washed 6 times with a 1.2 ml aliquot of Tris-binding buffer (pH 7.4), then air-dried and submerged in 5 ml of scintillation fluid (Ultima Gold XR, PerkinElmer). Liquid scintillation spectrometry was used to quantify radioactivity. For competition binding experiments, specific binding was equal to the difference in radioactivity with or without 1 µM unlabelled CP55,940.

Measurement of interleukins (IL-6 and IL-10) release in HMC3 cells

The concentrations of pro-inflammatory (IL-6) and anti-inflammatory (IL-10) interleukins were determined by performing specific ELISA assays (MyBioSource, San Diego,

TABLE 1 Inhibition of forskolin-stimulated cAMP and βarrestin2 recruitment.

Compound(s)	Inhibition of cAMP		βarrestin2 recruitment	
	EC_{50} (nM) (95% C.I.)	E_{max} (% CP55,940) ± S.E.M	EC_{50} (nM) (95% C.I.)	E_{max} (% CP55,940) ± S.E.M
CP55,940	9.4 (3.4–29)	100 ± 6.4	560 (410–760)	100 ± 3.4
EC-21a	>10,000	2.5 ± 0.53*	>10,000	1.4 ± 0.96*
LV62	58 (5.5–250)	110 ± 5.3	63 (49–82)*	65 ± 1.4*
10 nM LV62 + EC21a	4.3 (0.47–34)	104 ± 5.2	n.d	n.d
JR14a	150 (51–220)	41 ± 5.7*	25 (16–39)*	39 ± 0.93*
JR16a	350 (78–850)*	36 ± 8.6*	n.c	27 ± 4.2*
JR22a	62 (2.5–410)	38 ± 5.5*	>10,000	33 ± 3.1*
JR26a	110 (60–210)*	41 ± 5.1*	>10,000	39 ± 6.1*
JR58a	270 (36–440)*	45 ± 2.9*	>10,000	51 ± 2.8*
JR60a	770 (200–1,110)*	46 ± 4.4*	>10,000	36 ± 9.2*
JR61a	420 (14–630)	46 ± 1.7*	>10,000	34 ± 2.2*
JR64a	8.6 (5.9–12)	38 ± 0.74*	>10,000	45 ± 2.4*

hCB$_2$R activity was quantified for cAMP inhibition using the DiscoveRx HitHunter® assay (CHO-K1 hCB$_2$R) in cells treated with compounds for 90 min, and for βarrestin2 recruitment using the DiscoveRx PathHunter® assay (CHO-K1 hCB$_2$R) in cells treated with compounds for 90 min. Data were fit to a variable slope (3 parameter) non-linear regression in GraphPad (v. 9.0). Data are mean with 95% confidence interval (C.I.) (EC_{50}) or mean ± S.E.M. (E_{max}), n = 6 independent experiments performed in triplicate. Statistical analyses were by non-overlapping C.I. or two-way ANOVA followed by Bonferroni's post-hoc test. *$p < 0.05$ relative to CP55,940 within assay. n. d, not determined; n. c, not converged. E_{max} values for data that were not fit to a non-linear regression are the mean from the maximum value observed.

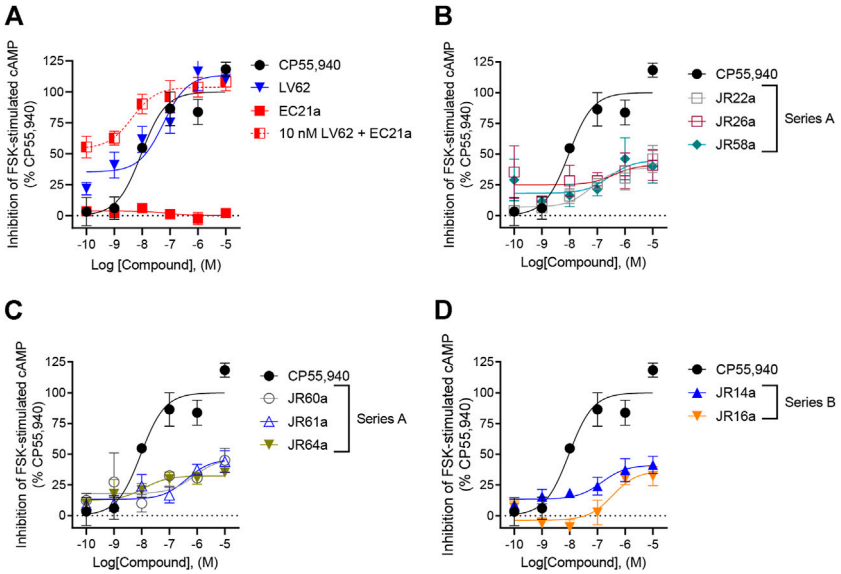

FIGURE 2
Evaluation of hCB$_2$R-dependent inhibition of FSK-stimulated cAMP. CHO cells stably-expressing hCB$_2$R were treated with 0.10 nM—10 μM compounds and 10 μM FSK for 90 min and cAMP inhibition was measured. **(A)** Parent compounds used for the design of the JR derivatives; **(B,C)** compounds of series **A**; **(D)** compounds of series **B**. CP55,940 data are the same in all four panels and presented for reference. Data are expressed as % CP55,940 response. Data were fitted to a non-linear regression (3 parameter model, GraphPad v. 9.0). Data are mean ± S.E.M. of six independent experiments performed in triplicate.

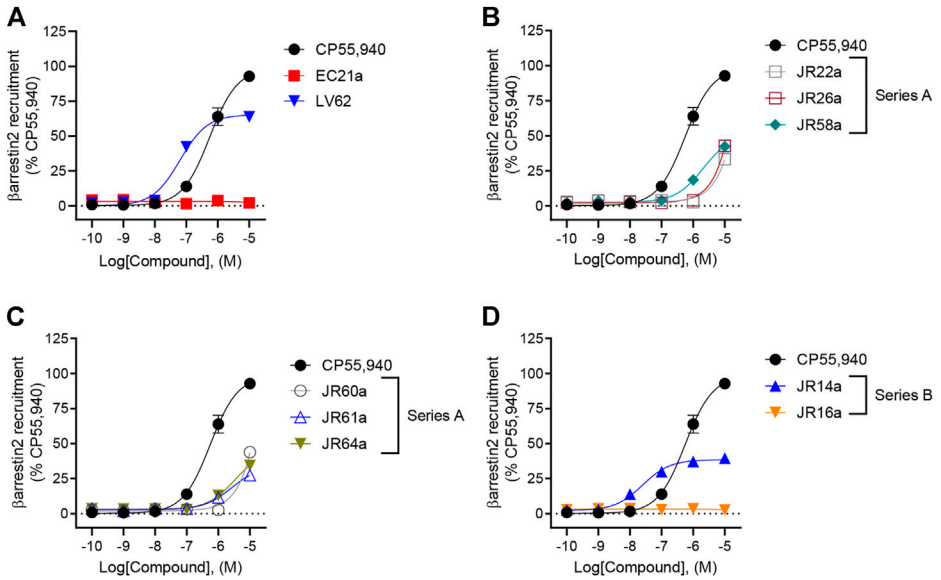

FIGURE 3
Evaluation of hCB$_2$R-dependent recruitment of βarrestin2. CHO-K1 cells stably-expressing hCB$_2$R were treated with 0.10 nM—10 μM compounds for 90 min and βarrestin2 recruitment was measured. **(A)** Parent compounds used for the design of the JR derivatives; **(B,C)** compounds of series **A**; **(D)** compounds of series **B**. CP55,940 data are the same in all four panels and presented for reference. Data are expressed as % CP55,940 response. Data were fitted to a non-linear regression (3 parameter model, GraphPad v. 9.0). Data are mean ± S.E.M. of six independent experiments performed in triplicate.

CA, United States) on collected culture media. Human microglial cells (HMC3) were exposed to pretreatment with test compounds for 1 h followed by stimulation with LPS (10 μg/ml)/TNFα (50 ng/ml) for 24 h. In competition experiments, the CB$_2$R antagonist (SR144528, 1 μM) or the CB$_2$R positive allosteric modulator (**EC21a** 1 or 10 μM) were administered 15 min before agonist administration.

Western blot analysis of CB2R expression in HMC3 cells

The expression of CB$_2$Rs was evaluated in human microglia cell lysates by Western blot experiments. Briefly, 50 μg of protein was diluted with Laemmli sample buffer 2×, boiled for 8 min at 96°C, separated on Criterion TGXTM gel (4–20%) and transferred into PVDF membranes. To avoid non-specific immunodetection, membranes were incubated for 45 min in T-TBS (20 mM Tris, 500 mM NaCl, 0.1% Tween-20, pH 8) containing 5% non-fat milk. Blots were then incubated overnight at 4°C with a rabbit anti- CB$_2$R antibody (#ab3561, Abcam, Cambridge, United Kingdom). Next, the membranes were incubated with HRP-labeled secondary anti-rabbit (#MAB201P, Merck-Millipore, Darmstadt, Germany) for 2 h at room temperature. Detection of chemiluminescence signals and densitometric analysis of blots were performed using ImageQuant LAS 4000 (GE Healthcare, Milan, Italy) and ImageLab software (Bio-Rad, Hercules, CA, United States), respectively.

Statistical analysis

Data for [^{3}H]CP55,940 binding are expressed as % of maximum [^{3}H]CP55,940 bound (i.e. 100%). HitHunter® cAMP, and PathHunter® βarrestin2 data are shown as % of maximal CP55,940 response (i.e. 100%). Concentration–response curves (CRC) were fit using non-linear regression (3 parameters) and used to calculate EC_{50}, E_{max}, or IC_{50} (GraphPad, Prism, v. 9.0). Statistical analyses were conducted by one-way analysis of variance (ANOVA), as indicated in the figure legends, using GraphPad. Post-hoc analyses were performed using Tukey's (one-way ANOVA) test. Homogeneity of variance was confirmed using Bartlett's test. All results are reported as the mean ± the standard error of the mean (SEM) or 95% confidence interval (CI), as indicated. $p_{values} < 0.05$ were considered significant.

Results and discussion

Chemistry

The synthesis of novel compounds, **JR14a**, **JR16a**, **JR22a**, **JR26a**, **JR58a**, **JR60a**, **JR61a** and **JR64a**, along with their corresponding precursors, was accomplished as depicted in Schemes 1-5.

As described in Scheme 1, the ethyl ester **1** (Manera et al., 2009) was dissolved in anhydrous DMF with the *p*-fluorobenzyl bromide in the presence of cesium carbonate at 50 °C for 12 h.

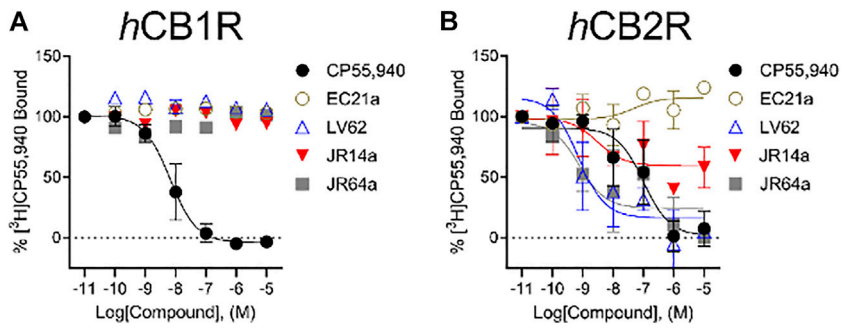

FIGURE 4
[^{3}H]CP55,940 binding to hCB$_1$R and hCB$_2$R. Membranes from CHO-K1 cells stably-expressing hCB$_1$R **(A)** or hCB$_2$R **(B)** were incubated with 1 nM [^{3}H]CP55,940 and 0.10 nM—10 μM compounds for 2 h. Data are expressed as % [^{3}H]CP55,940 bound. Data were fitted to a non-linear regression (3 parameter model to estimate changes in displacement [IC$_{50}$] which was substituted for EC$_{50}$, GraphPad v. 9.0). Data are mean ± S.E.M. of at least three independent experiments performed in duplicate. Data from these graphs is presented in Table 2.

TABLE 2 [^{3}H] CP55,940 binding.

Compound(s)	*h*CB1R		*h*CB2R	
	IC$_{50}$ (nM) (95% C.I.)	E_{min} (% CP55,940) ± S.E.M	IC$_{50}$ (nM) (95% C.I.)	E_{min} (% CP55,940) ± S.E.M
CP55,940	6.6 (2.7–15)	0.0 ± 5.6	40 (7.7–220)	1.5 ± 14.3
EC21a	n.c	103 ± 2.5***	36 (4.6–77)	115 ± 7.9***
LV62	n.c	106 ± 3.6***	0.65 (0.13–34)	16 ± 11.9
JR14a	n.c	98 ± 2.5***	1.8 (0.26–6.2)	59 ± 12.3*
JR64a	n.c	104 ± 4.7***	0.60 (0.20–26)	20 ± 10.3

Competition binding of [^{3}H]CP55,940 to hCB$_1$R and hCB$_2$R was quantified in membranes derived from CHO-K1 hCB1R or hCB2R cells incubated with compounds for 2 h. Data were fit to a three-parameter non-linear regression in GraphPad (v. 9.0). Data are mean with 95% C.I. (IC$_{50}$) or mean ± S.E.M, $n \geq 3$ independent experiments performed in duplicate. Statistical analyses were by non-overlapping C.I. or two-way ANOVA followed by Bonferroni's post-hoc test. *$p < 0.05$, ***$p < 0.001$ relative to CP55,940 within receptor. Data from this Table are graphed in Figure 4 n. c, not converged. E_{min} values for data that were not fit to a non-linear regression are the mean from the minimum value observed.

After this time and solvent removal, the crude product was immediately subjected to alkaline hydrolysis of ester group in the presence of NaOH al 10% at reflux for 24h, followed by acidification, affording the carboxylic acid **2**. The amide **3** was obtained by reaction of derivative **2** with *cis*-4-(Boc-amino) cyclohexylamine in the presence of TBTU, NEt$_3$, at room temperature for 12 h. The tert-butyl carbamate (BOC) deprotection of **3** was performed under acidic conditions by using CF$_3$COOH at −20°C for 3 h to yield the amino-derivative **4**. Finally, the derivative **4** was reacted with 5-azidopentanoic acid (previously prepared by reacting 5-bromovaleric acid, with NaN$_3$ in DMF at 60°C for 12 h) in the presence of TBTU according to the procedure described above, to afford the desired compound **5** (Scheme 1).

As reported in Scheme 2, the N1-alkylation of 1,8-naphthyridine-3-carboxamide **6** [(Manera et al., 2009) in anhydrous DMF with the suitable halogenated reagent in the presence of cesium fluoride afforded the desired 1,8-naphthyridin-2-one derivatives **7**, **9–11**. Additionally, compound **7** was also used as starting material in the presence of sodium azide at 60°C for 12 h to give compound **8**.

As reported in Scheme 3, the commercially available starting material 2-hydroxy-4-methyl-3-nitropyridine was treated with iron powder and ammonium chloride at 80°C for 3 h, to afford the amine compound **12**. The reaction between the amine derivative **12** and the cycloheptanecarbonyl chloride in DMF and triethylamine initially at 0°C and then at room temperature for 24 h, gave the amides **13**. The acyl chloride was prepared by reaction between cycloheptanecarboxylic acid and oxalyl chloride at room temperature for 30 min. The 5-bromo derivative **14** was obtained from compound **13** for treatment with Br$_2$ in CHCl$_3$ at room temperature for 12 h. Finally, compound **14** was subjected to a N-alkylation reaction by treatment with cesium fluoride in anhydrous DMF, at room temperature for 1 h and then with the suitable halogenated reagent at 50°C for 12 h, affording the desired alkyne derivatives **15** and **16**.

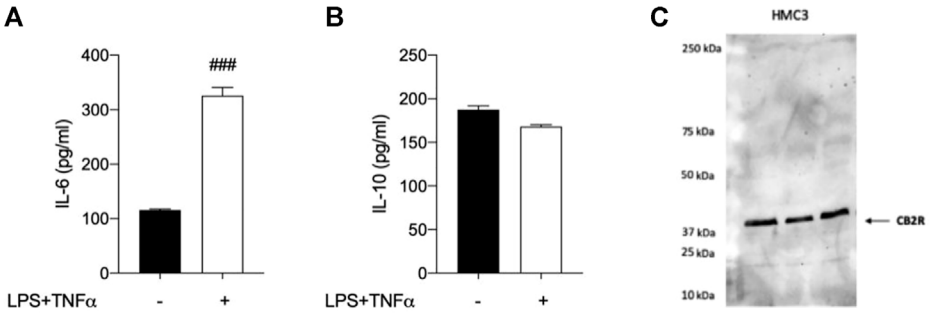

FIGURE 5
Analysis of HMC3 cell line response to inflammatory stimulus and expression of CB_2R. **(A)** Pro-inflammatory interleukin-6 (IL-6) and **(B)** anti-inflammatory interleukin-10 (IL-10) levels were measured after exposure to LPS (10 μg/ml)/TNFα (50 ng/ml) stimulus for 24 h. **(C)** Western Blot (WB) analysis allowed the detection of CB2R in control HMC3 cell lysates. [A-B]: data represent means ± S.E.M. from $n = 3$ independent experiments, performed in duplicate. Statistical analysis was performed by ordinary one-way ANOVA followed by Tukey's multiple comparison test. $^{###}p <$ 0.005 compared to control cells.

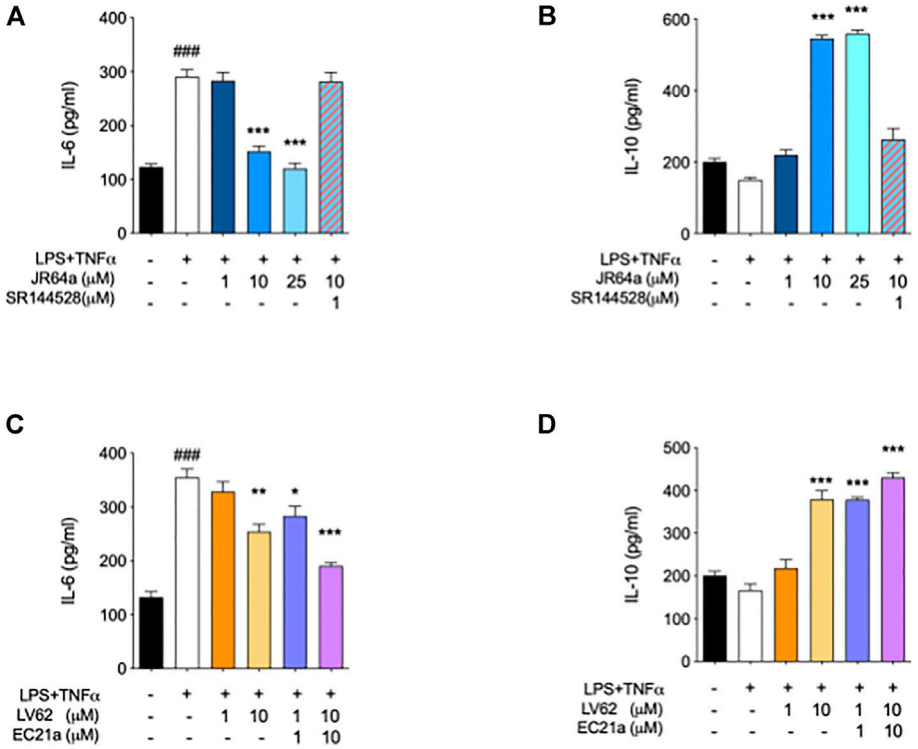

FIGURE 6
Ability of dualsteric CB_2R ligand **JR64a** to decrease the inflammatory phenotype of LPS/TNFα stimulated HMC3 cells. Panels **(A)** and **(B)** show the effects of **JR64a** on the release of pro-and anti-inflammatory interleukines IL-6 and IL-10, respectively. Panels **(C)** and **(D)** show the effects produced in the same experimental setting by administering CB_2R selective orthosteric agonist **LV62** alone or in combination (1:1) with the CB_2R PAM **EC21a**. Bars represent the release (pg/ml) of ILs in the presence of the compounds. Data represent mean ± SEM from $n = 3$ independent experiments performed in duplicate. Statistical analysis was performed by ordinary one-way ANOVA followed by Tukey's multiple comparison test. $^{###}p < 0.005$ vs. control cells; $^{*}p < 0.05$, $^{**}p < 0.01$ and $^{***}p < 0.005$ vs. LPS/TNFα treated cells.

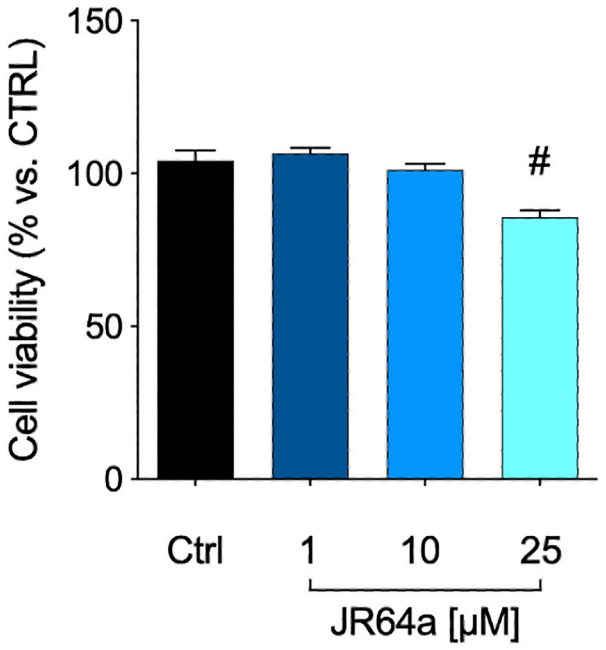

FIGURE 7
MTT assay performed with different concentrations of **JR64a**. Data represent means ± S.E.M. from n = 3 independent experiments, performed in triplicate. Statistical analysis was performed by ordinary one-way ANOVA followed by Tukey's multiple comparison test. $^{\#}p < 0.05$ vs. control.

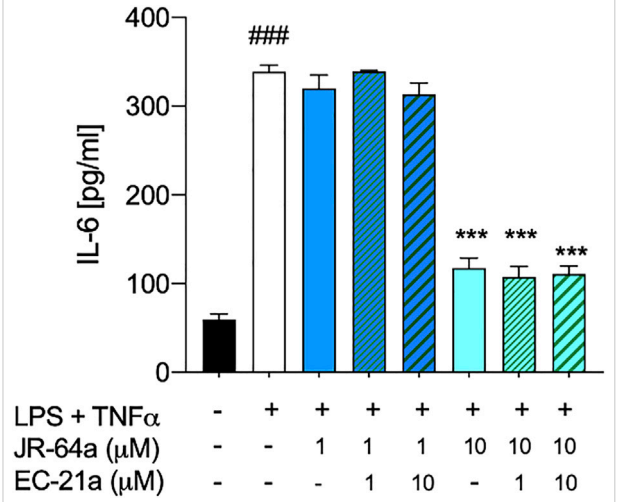

FIGURE 8
Co-administration of selective **CB_2R PAM EC21a** doesn't modify the effects of **JR64a** on the release of IL-6 in HMC3 cells exposed to LPS/TNFα stimulus. Bars represent the release (pg/ml) of IL-6 in the presence of the compounds. Data represent mean ± SEM from n = 3 independent experiments performed in duplicate. Statistical analysis was performed by ordinary one-way ANOVA followed by Tukey's multiple comparison test. $^{\#\#\#}p < 0.005$ vs. control cells; $^{***}p < 0.005$ vs. LPS/TNFα treated cells.

As showed in Scheme 4, the final compounds **JR14a** and **JR16a** were easily obtained by click chemistry reaction of the azido derivative **5** with the alkyne derivatives **15** or **16** in DMF and water in the presence of $CuSO_4.5H_2O$ and sodium ascorbate, at 80°C for 2 h. The same click reaction was also conducted between the azido derivative **7** with the alkyne derivatives **15** and **16** to afford the compounds **JR22a** and **JR26a.**

Finally, the synthesis of final compounds **JR58a**, **JR60a**, **JR61a** and **JR64a,** was accomplished as depicted in Scheme 5. The 5-bromo derivative **14** was subjected to a N-alkylation reaction by treatment with sodium hydride at 60% in anhydrous DME: DMF (4: 1, v/v) mixture, at 0°C for 15 min, followed by the addition of lithium bromide, at room temperature for 20 min, and then of the appropriate N1-alkylated intermediate **7, 9–11** at 65 °C for 12 h, affording, after purification, the desired compounds **JR58a**, **JR60a**, **JR61a** and **JR64a**.

$G\alpha_{i/o}$ protein-dependent inhibition of forskolin (FSK)-stimulated cAMP accumulation and ligand induced recruitment of βarrestin2

The new dualsteric CB_2R ligands of general chemical structure **A** (**JR22a**, **JR26a**, **JR58a**, **JR60a**, **JR61a**, and **JR64a**) and **B** (**JR14a**, **JR16a**), along with their relative parent compounds **EC21a** and **LV62,** were screened to assay their ability to inhibit FSK-stimulated cAMP accumulation in CHO-K1 cells stably-expressing $h$$CB_2R$ (Table 1). The non-selective orthosteric CBR ligand CP55,490 was used as a reference compound. Cells were treated with 10 μM FSK and CP55,490 or compound for 90 min to assess ligand concentration-dependent activity. Regarding the parent compounds, for **EC21a** no response was detected in accordance with its allosteric nature. **LV62** showed nanomolar potency (EC_{50} = 58 nM) and high relative efficacy (E_{max} = 110 ± 8.8) (Table 1; Figure 2A). The baseline for **LV62** was higher than that of CP55,940 (Figure 2A), indicating that E_{min} and E_{max} may be poorly defined within this assay, which may be a product of the curve fit for **LV62** or an artefact of the assay. In co-administration experiments, the activity of 10 nM **LV62** was augmented by **EC21a** in a concentration-dependent manner (EC_{50} = 4.3 nM) (Table 1; Figure 2A), confirming the role of **EC21a** as a CB_2R positive allosteric modulator (PAM) (Gado et al., 2019).

Among the compounds tested, **JR64a** and **JR14a**, were the most interesting of series **A** and **B** respectively (Table 1; Figure 2B). In particular **JR64a** was more potent than the orthosteric agonist **LV62** ($EC_{50(JR64a)}$ = 8.6 nM; $EC_{50(LV62)}$ = 58 nM [not statistically significant]); and its potency was also almost comparable to that observed in **EC21a** and **LV62** co-administration experiments ($EC_{50(LV62+EC21a)}$ = 4.3 nM). All

other tested **JR** compounds displayed lower potency compared to the parent orthosteric agonist **LV62** or the compounds **JR64a** (Table 1). Only a modest efficacy, ranging from 38 to 41%, and lower than that observed in **EC21a** and **LV62** co-administration experiments ($E_{max(LV62+EC21a)}$ = 104 ± 5.2), was observed for both **JR14a** and **JR64a** (Table 1). Therefore, the combination of **EC21a** (PAM) and **LV62** (agonist) produced greater potency and efficacy than the resultant **JR** compounds, obtained conjoining these two ligands. Nevertheless, our results indicated that the ligands **JR14a** and **JR64a** displayed modest partial agonist activity in the inhibition of FSK-stimulated cAMP accumulation assay in *h*CB_2R-expressing cells.

In addition to G protein-mediated signaling, GPCRs also interact with βarrestins, which facilitates receptor internalization, recycling, degradation, and signaling (Chen et al., 2014; Donthamsetti et al., 2020). Therefore, the complete panel of new orthosteric/allosteric hybrid CB_2R ligands and their corresponding parent compounds were evaluated for their ability to enhance βarrestin2 recruitment in CHO cells stably-expressing *h*CB_2R. Cells were treated with CP55,490 or compound for 90 min (Figure 3; Table 1). Regarding the parent compounds, no response was detected for **EC21a** alone, which is consistent with its activity as a CB_2R PAM (Figure 3A; Table 1). The CB_2R orthosteric agonist **LV62** enhanced βarrestin2 recruitment with both potency and efficacy comparable to those previously observed in FSK-stimulated cAMP accumulation assays (Table 1). Interestingly, analogs **JR14a** and **JR64a**, previously shown to inhibit FSK-stimulated cAMP accumulation, exhibited different behaviors in enhancing βarrestin2 recruitment (Figure 3; Table 1). **JR14a** enhanced βarrestin2 recruitment with nanomolar potency ($EC_{50(JR14a)}$ = 25 nM), whereas **JR64a**, did not significantly enhance βarrestin2 recruitment at concentrations below 10,000 nM. Therefore, **JR64a** displayed greater potency in the inhibition of cAMP accumulation as compared to the recruitment of βarrestin2 (biased ligand). This result may be important for the design of new CB_2R agonists devoid of the side effects related to the internalization and desensitization of CB_2Rs. Indeed, it has been reported that CB_2R agonists, by enhancing βarrestin2 recruitment, can induce internalization and desensitization of the receptor leading to a decrease in signaling and surface receptor levels (Chen et al., 2014).

[^{3}H]CP55,940 binding assays

Following characterization of G protein-mediated cAMP inhibition and βarrestin2 recruitment, we assessed ligand affinity for **LV62**, **EC21a**, **JR14a**, and **JR64a** at *h*CB_1R and *h*CB_2R using a [^{3}H]CP55,940 radioligand displacement assay on membranes derived from CHO-K1 cells stably-expressing either receptor. No affinity at *h*CB_1R was detected for all compounds (Figure 4A; Table 2). At *h*CB_2R, consistent with its CB_2R PAM character, **EC21a** increased [^{3}H]CP55,940 bound to *h*CB_2R (Figure 4B; Table 2). **LV62** fully displaced [^{3}H]CP55,940 from *h*CB_2R, as expected for an orthosteric compound (Figure 4B; Table 2). Remarkably, novel *h*CB_2R ligands **JR14a** and **JR64a** displayed nanomolar relative affinities in the [^{3}H]CP55,940 displacement assay with *h*CB_2R CHO-K1 cell membranes (Figure 4B; Table 2; $IC_{50(JR14a)}$ = 1.8 nM; $IC_{50(JR64a)}$ = 0.60 nM).

Anti-inflammatory properties of selected CB_2R ligands in human microglial cells (HMC3)

Taking into account that the inflammatory process in microglial cells supports the onset and progression of several neurodegenerative and psychiatric disorders (Nakagawa and Chiba, 2014; Hansen et al., 2018; Haukedal and Freude 2019; Ho 2019), we decided to investigate the anti-inflammatory properties of novel CB_2R ligand **JR64a**, which had emerged from a preliminary screening as the most promising of the series. At this aim, we first set up a human model of microglial inflammation, by exposing HMC3 cells to LPS/TNFα stimulus (Dello Russo et al., 2018). In agreement with our previous observations (Polini et al., 2020; Gado et al., 2022), exposure of microglial cells to LPS/TNFα resulted in a significant increase of the release of pro-inflammatory IL-6 as compared to control cells (Figure 5A), whereas no significant effects were observed on IL-10 release (Figure 5B). Expression of CB_2R in HMC3 microglial cells was also assessed by WB analysis (Figure 5C). Then, dose-response experiments were carried out by exposing HMC3 cells to pretreatment with increasing concentrations (1, 10, and 25 μM) of test compound followed by LPS/TNFα treatment for 24 h (Figure 6). Notably, no relevant cytotoxic effects were detected in HMC3 cells after treatment with **JR64a** at 1 and 10 μM concentrations (Figure 7), whereas when used at 25 μM a modest decrease in cell viability (ca 10%) was observed (Figure 7). Measurements of pro- and anti-inflammatory interleukins levels (i.e. IL-6 and IL-10) in cell media by ELISA tests revealed that, when used at 10 or 25 μM concentration, analog **JR64a** displayed a marked anti-inflammatory activity, which was completely abolished after pretreatment with the CB_2R selective antagonist **SR144528** (1 μM, Figures 6A,B), suggesting a CB_2R-mediated anti-inflammatory effect in HMC3 microglial cells. In parallel experiments, the anti-inflammatory effects of the orthosteric agonist **LV62** administered at 1 or 10 μM concentration either individually or in equimolar combination with the CB_2R-PAM **EC21a** were evaluated. As shown in Figures 6C,D,

administration of **EC21a** at equimolar dosages enhanced **LV62** anti-inflammatory activity, which resulted in a similar response to that observed on administration of equimolar concentrations of the hybrid compound **JR64a** (Figures 6A,B). Notably, co-administration of **EC21a** at equimolar or higher doses revealed no effects on **JR64a** anti-inflammatory activity in HMC3 cells (Figure 8), suggesting a potential ability for **JR64a** to interact with both orthosteric and allosteric sites of CB_2R. However, additional investigation is needed to confirm the potential bitopic pharmacology of **JR64a**. In particular, computational studies using our recently proposed model of CB_2R in complex with bitopic ligands (Gado et al., 2022) could certainly help to clarify the binding mode of **JR64a** and its ability of occupying both orthosteric and allosteric site of the CB_2R, as well as to facilitate the rational design of novel and more effective CB_2R bitopic ligands.

Conclusion

Recent progress made in the discovery and functional characterization of GPCRs ligands have enabled the design of bitopic/duasteric ligand as single chemical entities in which an orthosteric and an allosteric pharmacophore are chemically attached via a linker in a manner to allow simultaneous targeting of two binding sites (orthosteric and allosteric) within one receptor. This approach may offer several advantages over the classical 'monovalent' ligand, such as an increased affinity and selectivity for the target receptor, often accompanied with functional selectivity (stimulus bias) (Newman et al., 2020). However, the design of bitopic ligands needs deep knowledge of orthosteric and allosteric ligands for a given GPCR as well as its binding sites (orthosteric and allosteric.). For these reasons, bitopic ligands have so far been described predominantly for muscarinic receptors (Valant, et al., 2008; Keov, et al., 2014), adenosine receptors (Valant et al., 2014), and dopamine receptors (Draper-Joyce et al., 2018), for which detailed knowledge on allosteric binding sites and ligands is available.

In this study we have presented the synthesis and functional characterization of novel potential CB_2R dualsteric agents, designed as hybrid compounds composed of two distinct pharmacophoric units, namely the CB_2R PAM **EC21a** and the CB_2R orthosteric agonist **LV62,** linked through different alkyl chains. After a preliminary screening, which included $G\alpha_{i/o}$ protein-dependent inhibition of FSK-stimulated cAMP accumulation, ligand induced recruitment of βarrestin2, and binding to hCB$_2$R, analog **JR64a** was identified as the most promising dualsteric CB_2R ligand. Indeed, a bias towards the modulation of the cAMP-pathway over the recruitment of βarrestin2 combined with high affinity for binding to hCB$_2$R were observed. Subsequently, the lead compound was tested to evaluate its ability to decrease the inflammatory phenotype of LPS/TNFα-stimulated human microglial cells (HMC3). Our results indicated that analog **JR64a** displayed good anti-inflammatory properties when used at 10 μM concentration. Notably, as demonstrated by pharmacological antagonism, the anti-inflammatory effect displayed by **JR64a** revealed to be CB_2R-mediated, and no relevant HMC3 cytotoxicity was also observed after administering **JR64a** at 10 μM concentration. Even though still at a preliminary level, functional assays indicated that the selective CB_2R PAM analog **EC21a** was not able to increase the anti-inflammatory effects produced by **JR64a** in HMC3 cells, supporting the design of this compound as a potential CB_2R dualsteric ligand. Certainly, the availability of dualsteric/bitopic ligands for the CB_2R can provide a fundamental contribution to the clarification of the mechanism of action of this receptor. It is therefore essential to provide an unequivocal demonstration of a simultaneous allosteric/orthosteric mode of binding for new bitopic ligand candidates. The good news is that recent advances in CB_2R structural biology might help in the construction of allosteric/bitopic ligands with a designed pharmacological profile. Therefore, future structural and functional studies will provide critical insights to confirm the actual CB_2R-bitopic ligand behavior of our novel analog **JR64a**.

Data availability statement

The original contributions presented in the study are included in the article/Supplementary Material, further inquiries can be directed to the corresponding authors.

Author contributions

GC, CM, RL, and RP conceived and designed the experiments. CM, RF, FG, GS, SR and GO performed the design, synthesis, and chemical characterization of all novel compounds. KM, LS, RF, RP, and RL carried out cAMP, βarrestin2, and radioligand displacement assays. BP, CR, FG and GC performed the interleukins release experiments. GC, CM, RP, and RL analysed the results. GC, CM and RL wrote the paper. All authors verified the data, contributed to the manuscript, and approved the final version.

Funding

This work was supported by University of Pisa Research Grant (PRA_2020_77), by Italian Ministry of Health–Ricerca Finalizzata 2016—NET-2016-02363765, by a CIHR-GSK partnership grant and an NSERC discovery grant to RL. KM is supported by an NSERC National graduate student award.

Conflict of interest

The authors declare that the research was conducted in the absence of any commercial or financial relationships that could be construed as a potential conflict of interest.

Publisher's note

All claims expressed in this article are solely those of the authors and do not necessarily represent those of their affiliated organizations, or those of the publisher, the editors and the reviewers. Any product that may be evaluated in this article, or claim that may be made by its manufacturer, is not guaranteed or endorsed by the publisher.

Supplementary Material

The Supplementary Material for this article can be found online at: https://www.frontiersin.org/articles/10.3389/fchem.2022.984069/full#supplementary-material

References

Antony, J., Kellershohn, K., Mohr-Andrä, M., Kebig, A., Prilla, S., Muth, M., et al. (2009). Dualsteric GPCR targeting: A novel route to binding and signaling pathway selectivity. *FASEB J.* 23, 442–450. doi:10.1096/fj.08-114751

Aymerich, M. S., Aso, E., Abellanas, M. A., Tolon, R. M., Ramos, J. A., Ferrer, I., et al. (2018). Cannabinoid pharmacology/therapeutics in chronic degenerative disorders affecting the central nervous system. *Biochem. Pharmacol.* 157, 67–84. doi:10.1016/j.bcp.2018.08.016

Basavarajappa, B. S., Nixon, R. A., and Arancio, O. (2009). Endocannabinoid system: Emerging role from neurodevelopment to neurodegeneration. *Mini Rev. Med. Chem.* 9, 448–462. doi:10.2174/138955709787847921

Benito, C., Kim, W. K., Chavarria, I., Hillard, C. J., Mackie, K., Tolon, R. M., et al. (2005). A glial endogenous cannabinoid system is upregulated in the brains of macaques with simian immunodeficiency virus-induced encephalitis. *J. Neurosci.* 25, 2530–2536. doi:10.1523/JNEUROSCI.3923-04.2005

Benito, C., Nunez, E., Tolon, R. M., Carrier, E. J., Rabano, A., Hillard, C. J., et al. (2003). Cannabinoid CB2 receptors and fatty acid amide hydrolase are selectively overexpressed in neuritic plaque-associated glia in Alzheimer's disease brains. *J. Neurosci.* 23, 11136–11141. doi:10.1523/JNEUROSCI.23-35-11136.2003

Bie, B., Wu, J., Foss, J.F., and Naguib, M. (2018). An overview of the cannabinoid type 2 receptor system and its therapeutic potential. *Curr. Opin. Anaesthesiol.* 31, 407–414. doi:10.1097/ACO.0000000000000616

Bisogno, T., Ligresti, A., and Di Marzo, V. (2005). The endocannabinoid signalling system: Biochemical aspects. *Pharmacol. Biochem. Behav.* 81, 224–238. doi:10.1016/j.pbb.2005.01.027

Bock, A., and Bermudez, M. (2021). Allosteric coupling and biased agonism in G protein-coupled receptors. *FEBS J.* 288, 2513–2528. doi:10.1111/febs.15783

Chen, X., Zheng, C., Qian, J., Sutton, S. W., Wang, Z., Lv, J., et al. (2014). Involvement of β-arrestin-2 and clathrin in agonist-mediated internalization of the human cannabinoid CB2 receptor. *Curr. Mol. Pharmacol.* 7, 67–80. doi:10.2174/1874467207666140714115824

Chung, Y. C., Shin, W. H., Baek, J. Y., Cho, E. J., Baik, H. H., Kim, S. R., et al. (2016). CB2 receptor activation prevents glial-derived neurotoxic mediator production, BBB leakage and peripheral immune cell infiltration and rescues dopamine neurons in the MPTP model of Parkinson's disease. *Exp. Mol. Med.* 48, e205. doi:10.1038/emm.2015.100

Cooper, A. G., Oyagawa, C. R. M., Manning, J. J., Singh, S., Hook, S., Grimsey, N. L., et al. (2018). Development of selective, fluorescent cannabinoid type 2 receptor ligands based on a 1, 8-naphthyridin-2-(1*H*)-one-3-carboxamide scaffold. *Medchemcomm* 9, 2055–2067. doi:10.1039/c8md00448j

Dello Russo, C., Cappoli, N., Coletta, I., Mezzogori, D., Paciello, F., Pozzoli, G., et al. (2018). The human microglial HMC3 cell line: Where do we stand? A systematic literature review. *J. Neuroinflammation* 15, 259. doi:10.1186/s12974-018-1288-0

Di Marzo, V. (2009). The endocannabinoid system: Its general strategy of action, tools for its pharmacological manipulation and potential therapeutic exploitation. *Pharmacol. Res.* 60, 77–84. doi:10.1016/j.phrs.2009.02.010

Donthamsetti, P., Gallo, E. F., Buck, D. C., Stahl, E. L., Zhu, Y., Lane, J. R., et al. (2020). Arrestin recruitment to dopamine D2 receptor mediates locomotion but not incentive motivation. *Mol. Psychiatry* 25, 2086–2100. doi:10.1038/s41380-018-0212-4

Draper-Joyce, C. J., Michino, M., Verma, R. K., Klein Herenbrink, C., Shonberg, J., Kopinathan, A., et al. (2018). The structural determinants of the bitopic binding mode of a negative allosteric modulator of the dopamine D2 receptor. *Biochem. Pharmacol.* 148, 315–328. doi:10.1016/j.bcp.2018.01.002

Ferrisi, R., Ceni, C., Bertini, S., Macchia, M., Manera, C., and Gado, F. (2021). Medicinal Chemistry approach, pharmacology and neuroprotective benefits of CB2R modulators in neurodegenerative diseases. *Pharmacol. Res.* 170, 105607. doi:10.1016/j.phrs.2021.105607

Gado, F., Di Cesare Mannelli, L., Lucarini, E., Bertini, S., Cappelli, E., Digiacomo, M., et al. (2019). Identification of the first synthetic allosteric modulator of the CB2 receptors and evidence of its efficacy for neuropathic pain relief. *J. Med. Chem.* 62, 276–287. doi:10.1021/acs.jmedchem.8b00368

Gado, F., Ferrisi, R., Polini, B., Mohamed, K. A., Ricardi, C., Lucarini, E., et al. (2022). Design, synthesis, and biological activity of new CB2 receptor ligands: From orthosteric and allosteric modulators to dualsteric/bitopic ligands. *J. Med. Chem.* 65, 9918–9938. doi:10.1021/acs.jmedchem.2c00582

Gado, F., Mohamed, K. A., Meini, S., Ferrisi, R., Bertini, S., Digiacomo, M., et al. (2021). Variously substituted 2-oxopyridine derivatives: Extending the structure-activity relationships for allosteric modulation of the cannabinoid CB2 receptor. *Eur. J. Med. Chem.* 211, 113116. doi:10.1016/j.ejmech.2020.113116

Garai, S., Kulkarni, P. M., Schaffer, P. C., Leo, L. M., Brandt, A. L., Zagzoog, A., et al. (2020). Application of fluorine and nitrogen-walk approaches: Defining the structural and functional diversity of 2-phenylindole class of cannabinoid 1 receptor positive allosteric modulators. *J. Med. Chem.* 63, 542–568. doi:10.1021/acs.jmedchem.9b01142

Gentry, P. R., Sexton, P. M., and Christopoulos, A. (2015). Novel allosteric modulators of G protein- coupled receptors. *J. Biol. Chem.* 290, 19478–19488. doi:10.1074/jbc.R115.662759

Gurevich, V. V., and Gurevich, E. V. (2019). The structural basis of the arrestin binding to GPCRs. *Mol. Cell. Endocrinol.* 484, 34–41. doi:10.1016/j.mce.2019.01.019

Han, S., Jayant Thatte, J., Buzard, D. J., and Jones, R. M. (2013). Therapeutic utility of cannabinoid receptor type 2 (CB2) selective agonists. *J. Med. Chem.* 56, 8224–8256. doi:10.1021/jm4005626

Hansen, D. V., Hanson, J. E., and Sheng, M. (2018). Microglia in Alzheimer's disease. *J. Cell. Biol.* 217, 459–472. doi:10.1083/jcb.201709069

Haukedal, H., and Freude, K. (2019). Implications of microglia in amyotrophic lateral sclerosis and frontotemporal dementia. *J. Mol. Biol.* 431, 1818–1829. doi:10.1016/j.jmb.2019.02.004

Ho, M. S. (2019). Microglia in Parkinson's disease. *Adv. Exp. Med. Biol.* 1175, 335–353. doi:10.1007/978-981-13-9913-8_13

Howlett, A. C., Barth, F., Bonner, T. I., Cabral, G., Casellas, P., Devane, W. A., et al. (2002). International union of pharmacology. XXVII. Classification of cannabinoid receptors. *Pharmacol. Rev.* 54, 161–202. doi:10.1124/pr.54.2.161

Kamal, M., and Jockers, R. (2009). Bitopic ligands: All-in-one orthosteric and allosteric. *F1000 Biol. Rep.* 1, 77. doi:10.3410/B1-77

Keov, P., Lopez, L., Devine, S. M., Valant, C., Lane, J. R., Scammells, P. J., et al. (2014). Molecular mechanisms of bitopic ligand engagement with the M1 muscarinic acetylcholine receptor. *J. Biol. Chem.* 289, 23817–23837. doi:10.1074/jbc.M114.582874

Lane, J. R., Sexton, P. M., and Christopoulos, A. (2013). Bridging the gap: Bitopic ligands of G-protein-coupled receptors. *Trends Pharmacol. Sci.* 34, 59–66. doi:10.1016/j.tips.2012.10.003

Li, X., Hua, T., Vemuri, K., Ho, J. H., Wu, Y., Wu, L., et al. (2019). Crystal structure of the human cannabinoid receptor CB2. *Cell.* 76, 459–467.e13. e13. doi:10.1016/j.cell.2018.12.011

Lucchesi, V., Hurst, D. P., Shore, D. M., Bertini, S., Ehrmann, B. M., Allarà, M., et al. (2014). CB2-selective cannabinoid receptor ligands: Synthesis, pharmacological evaluation, and molecular modeling investigation of 1, 8-naphthyridin-2(1*H*)-one-3-carboxamides. *J. Med. Chem.* 21, 8777–8791. doi:10.1021/jm500807e

Mackie, K. (2005). Distribution of cannabinoid receptors in the central and peripheral nervous system. *Handb. Exp. Pharmacol.* 2005, 299–325. doi:10.1007/3-540-26573-2_10

Manera, C., Saccomanni, G., Adinolfi, B., Benetti, V., Ligresti, A., Cascio, M. G., et al. (2009). Rational design, synthesis, and pharmacological properties of new 1, 8-naphthyridin-2(1H)-on-3-carboxamide derivatives as highly selective cannabinoid-2 receptor agonists. *J. Med. Chem.* 52, 3644–3651. doi:10.1021/jm801563d

Mastinu, A., Premoli, M., Ferrari-Toninelli, G., Tambaro, S., Maccarinelli, G., Memo, M., et al. (2018). Cannabinoids in health and disease: Pharmacological potential in metabolic syndrome and neuroinflammation. *Horm. Mol. Biol. Clin. Investig.* 36,/j/hmbci.2018.36.issue-2/hmbci-2018-0013/hmbci-2018-0013.xml. doi:10.1515/hmbci-2018-0013

Meijer, F. A., Oerlemans, G. J. M., and Brunsveld, L. (2021). Orthosteric and allosteric dual targeting of the nuclear receptor RORγt with a bitopic ligand. *ACS Chem. Biol.* 16, 510–519. doi:10.1021/acschembio.0c00941

Nakagawa, Y., and Chiba, K. (2014). Role of microglial M1/M2 polarization in relapse and remission of psychiatric disorders and diseases. *Pharmaceuticals* 7, 1028–1048. doi:10.3390/ph7121028

Newman, A. H., Battiti, F. O,, and Bonifazi, A. (2020). 2016 philip S. Portoghese medicinal chemistry lectureship: Designing bivalent or bitopic molecules for G-protein coupled receptors. The whole is greater than the sum of its parts. *J. Med. Chem.* 63, 1779–1797. doi:10.1021/acs.jmedchem.9b01105

Obeng, S., Hiranita, T., León, F., McMahon, L. R., and McCurdy, C. R. (2021). Novel approaches, drug candidates, and targets in pain drug discovery. *J. Med. Chem.* 64, 6523–6548. doi:10.1021/acs.jmedchem.1c00028

Oláh, A., Szekanecz, Z., and Bíró, T. (2017). Targeting cannabinoid signaling in the immune system: "High"-ly exciting questions, possibilities, and challenges. *Front. Immunol.* 8, 1487. doi:10.3389/fimmu.2017.01487

Polini, B., Cervetto, C., Carpi, S., Pelassa, S., Gado, F., Ferrisi, R., et al. (2020). Positive allosteric modulation of CB1 and CB2 cannabinoid receptors enhances the neuroprotective activity of a dual CB1R/CB2R orthosteric agonist. *Life* 333, 333–414. doi:10.3390/life10120333

Ramirez, S. H., Hasko, J., Skuba, A., Fan, S., Dykstra, H., McCormick, R., et al. (2012). Activation of cannabinoid receptor 2 attenuates leukocyte-endothelial cell interactions and blood-brain barrier dysfunction under inflammatory conditions. *J. Neurosci.* 32, 4004–4016. doi:10.1523/JNEUROSCI.4628-11.2012

Reinecke, B. A., Wang, H., and Zhang, Y. (2019). Recent advances in the drug discovery and development of dualsteric/bitopic activators of G protein-coupled receptors. *Curr. Top. Med. Chem.* 19, 2378–2392. doi:10.2174/1568026619666191009164609

Schrage, R., and Kostenis, E. (2017). Functional selectivity and dualsteric/bitopic GPCR targeting. *Curr. Opin. Pharmacol.* 32, 85–90. doi:10.1016/j.coph.2016.12.001

Shapiro, L., Gado, F., Manera, C., and Escayg, A. (2021). Allosteric modulation of the cannabinoid 2 receptor confers seizure resistance in mice. *Neuropharmacology* 188, 108448. doi:10.1016/j.neuropharm.2021.108448

Smith, J. S., Lefkowitz, R. J., and Rajagopal, S. (2018). Biased signalling: From simple switches to allosteric microprocessors. *Nat. Rev. Drug Discov.* 17, 243–260. doi:10.1038/nrd.2017.229

Steinfeld, T., Mammen, M., Smith, J. A. M., Wilson, R. D., and Jasper, J. R. (2007). A novel multivalent ligand that bridges the allosteric and orthosteric binding sites of the M2 muscarinic receptor. *Mol. Pharmacol.* 72, 291–302. doi:10.1124/mol.106.033746

Valant, C., Gregory, K. J., Hall, N. E., Scammells, P. J., Lew, M. J., Sexton, P. M., et al. (2008). A novel mechanism of G protein-coupled receptor functional selectivity. *J. Biol. Chem.* 283, 29312–29321. doi:10.1074/jbc.M803801200

Valant, C., May, L. T., Aurelio, L., Chuo, C. H., White, P. J., Baltos, J. A., et al. (2014). Separation of on-target efficacy from adverse effects through rational design of a bitopic adenosine receptor agonist. *Proc. Natl. Acad. Sci. U. S. A.* 111, 4614–4619. doi:10.1073/pnas.1320962111

Walter, L., Franklin, A., Witting, A., Wade, C., Xie, Y., Kunos, G., et al. (2003). Nonpsychotropic cannabinoid receptors regulate microglial cell migration. *J. Neurosci.* 23, 1398–1405. doi:10.1523/JNEUROSCI.23-04-01398.2003

Wootten, D., Christopoulos, A., and Sexton, P. M. (2013). Emerging paradigms in GPCR allostery: Implications for drug discovery. *Nat. Rev. Drug Discov.* 12, 630–644. doi:10.1038/nrd4052

Xu, J., Tang, Y., Xie, M., Bie, B., Wu, J., Yang, H., et al. (2016). Activation of cannabinoid receptor 2 attenuates mechanical allodynia and neuroinflammatory responses in a chronic post-ischemic pain model of complex regional pain syndrome type I in rats. *Eur. J. Neurosci.* 44, 3046–3055. doi:10.1111/ejn.13414

Zagzoog, A., Mohamed, K. A., Kim, H. J. J., Kim, E. D., Frank, C. S., et al. (2020). *In vitro* and *in vivo* pharmacological activity of minor cannabinoids isolated from Cannabis sativa. *Sci. Rep.* 10, 20405. doi:10.1038/s41598-020-77175-y